Engineering Structures 293 (2023) 116635

Contents lists available at ScienceDirect

Engineering Structures

journal homepage: www.elsevier.com/locate/engstruct

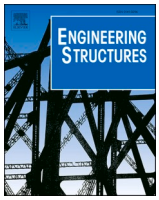

A new simplified approach for predicting the bearing capacity of rectangular concrete four-pile caps

Ridha Boulifa [a,b,*], Kamel Goudjil [a,b], Mohamed Laid Samai [c]

[a] Department of Civil Engineering, Mohamed Cherif Messaadia University, Souk-Ahras, Algeria
[b] Mohammed Cherif Messaadia University, Laboratory INFRARES, Souk-Ahras, Algeria
[c] Department of Civil Engineering, Faculty of Sciences of Technology, Mentouri Brothers University, Constantine, Algeria

ARTICLE INFO

Keywords:
Pile caps
Tow-dimensional Strut-and-Tie Model
Shear failure
Flexural failure
Concrete strut

ABSTRACT

Strut and tie models are mainly used to predict the critical failure mode of RC pile caps. The bearing capacity is determined by taking the lowest between flexural strength corresponding to reinforcement yielding and punching shear load of the concrete struts. However, the concrete-reinforcement interaction presents a key parameter for predicting failure mode and load-bearing capacity of rectangular four pile caps. The objective of the present study is to evaluate the strength capacity of RC pile caps by developing a simplified approach given by a unique equation considering both contributions of concrete and reinforcement corresponding to the failure mode. The proposed analytical approach considers the weakest coefficient of variation of (P_{test}/P_{model}) using the experimental database selected by the observed failure mechanism (flexion or shear) to evaluate the combination of the contributions ratios; of steel and concrete. The results are on the safe side (min (P test/ P model) = 1) and improved with lower scatter when compared to design methods from the literature (COV = 8.8% for all failure modes) and CRSI Handbook code.

1. Introduction

Pile caps are connecting elements that transmit the load from a column or a wall to a group of concrete piles; they serve as an interface between the superstructure and the substructure. Pile caps are subjected to concentrated loads and have large dimensions in all three directions, resulting in highly nonlinear strain distributions. Because pile caps are mostly disturbed regions, the utility of using sectional approaches based on empirical formulas for flexural elements is called into question.

The strut-and-tie model, based on the lower bound theorem of the theory of plasticity, has been developed in recent decades to provide a consistent alternative for the design of disturbed regions. The Concrete pile caps must be designed to resist the shear intensity load. The failure mode is governed by the potential diagonal crack between the column's perimeter and the vicinity of piles or other types of deep foundations.

Following the diagonal tension crack, the concrete footing equilibrated the punching load by the shear across the compression zone, aggregate interlock, and the dowel action of the flexural reinforcement [1]. However, many researchers like Meléndez et al. [2], Boulifa et al. [3], and Honglei Guo [4] are proven the primordial effect of the strength of confined inclined concrete struts on the load-carrying capacity of reinforced concrete pile caps failing without yielding the reinforcements. On the other hand, the design of pile caps to fail in flexure mode is very common in published experimental campaigns [5–7,8–11]. This type of failure is identified by forming a conical plug underneath the column or punching around one or more piles.

In the scientific literature devoted to the analysis and design of pile caps, most of the proposed analytical approaches are based on three-dimensional strut-and-tie models [2,7,12–16]; some of these models are reviewed in this paper. Most of these references focus on determining the bearing capacity of pile caps by considering only the characteristics and geometry of concrete for the case of shear failure mode [13,15] or by considering the yielding reinforcement without the contribution of concrete for the case of flexural failure mode [17]. Nevertheless, the minimum coefficient of variation (COV) of the results of the set of these models proposed so far is higher than 10% for all the grouped failure modes [2–4,13–17].

This study thoroughly analyzed the geometrical key parameters corresponding to the concrete and reinforcements for accurately predicting the bearing capacity based on the background of the most used experimental tests in the literature [6,8–11]. The analysis of variation of the coefficient of variation of the results in terms of ratio (P_{test}/P_{model})

* Corresponding author.
E-mail address: r.boulifa@univ-soukahras.dz (R. Boulifa).

https://doi.org/10.1016/j.engstruct.2023.116635
Received 22 January 2023; Received in revised form 2 July 2023; Accepted 17 July 2023
Available online 23 July 2023

for each experimental failure mode allows us to separately determine the contributions of the reinforcements and the concrete corresponding to the failure mode (by bending or by shear). The analytical model proposed in this work, which offers development on the sectional model presented in previous research [3], considers the effect of reinforcement in the shear failure mode and highlights the contribution of the confined concrete in the bending failure mode. The proposed analytical model allows determining precisely the bearing capacity of the four pile caps, considering the minimum value between the prediction for flexural failure and shear failure (coefficient of variation (COV) = 8.6% for all modes failure with min (P_{test}/P_{model}) = 1).

Before presenting the model under consideration in this study, it is necessary to present the experimental four pile caps database (107 test results), primarily presented in the published literature [6,8–11], and a discussion of the recent approaches and models used for predicting the bearing capacity of four pile caps.

2. Experimental data for pile caps

There are some limitations in the experimental test data on the pile caps' performance. Unfortunately, as the reinforcement patterns used in the test pile caps are incompatible with the design procedures, an essential portion of these results do not help assess these code provisions. In the case of four-pile caps, the reinforcement arrangement directly influences the failure mechanism. The results of several tests [6] have shown that the reinforcement with bunched square configurations (Fig. 1-a) leads to a capacity (20%) more significant than that of the specimens with reinforcement distributed in Grid pattern layouts. However, in the cases of deep pile caps, the failure occurs by the punching shear mechanism, forming a diagonal splitting crack in the midpart of the strut. The bunched square reinforcement layout can ensure only the confinement in the bottom zone. This type of reinforcement is the best suited for determining Strength Predictions for a 3-Dimensional Concrete Strut.

Clarke J. L. [6] tested 13 half-scale four-pile caps (Table 1) with reinforcement layouts in Fig. 1, where the specimens are designed to fail in flexure mode. He concluded that the approach based on analyzing the shear section for shear capacity calculations was unsafe. The flexural failure occurred only in four caps, whereas shear failure occurred in the remaining caps after the yielding of longitudinal reinforcement. Clarke J. L. [6] concluded that adequate depth must be considered for shear strength calculations. Suzuki et al. [8] tested 28 four-pile caps in which the layouts of the longitudinal bars and edge distances were varied. The different dimensions are given in Table 2. Most pile caps failed by shear after longitudinal reinforcement yielding, and only four specimens failed by shear without longitudinal reinforcement yielding. It was found that bunched square layouts (shown in Fig. 1) resulted in higher strengths and that the distance of the edge affected the load of failure. The edge distance was suggested to be about 1.5 times the diameter of the pile to increase deformation and load-bearing capacity even after yielding reinforcement. Later, Suzuki et al. [9] tested 18 four-pile caps with tapered footings (with top inclined slabs) (Table 2) and proved that cracking load tends to decrease as the ratio of reinforcement increases. In these experiments, most specimens failed in shear after longitudinal reinforcement yielding, and only two failed by shear before yielding reinforcement. Suzuki et al. [10] tested thirty pile caps where a grid layout assured the reinforcement; the dimensions of the specimens are given in Table 2. The main aim of the research was to evaluate the edge distance effect between the cap and the piles on behavior and strength. The results have shown that the load of the first crack and the flexural capacity decreases even if the slab reinforcement is the same when shortening the edge distance. Suzuki and Otsuki [11] tested eighteen four pile caps with grid reinforcement. The test parameters involved the type of anchorage and concrete strength (see Table 2). In most pile caps, the failure mode was due to the shear after the bottom reinforcement's yielding.

In contrast, all specimens were designed to fail by flexure. Ten of them did not fail by flexure. They concluded that this was due to the effect of shortened edge distances on the failure by shear. Short edge distances directly influence longitudinal reinforcement development. It can be concluded that the pile caps' failure occurs when there is yielding for either the tensioned tie or the compressed struts. So in the presence of suitable containment, the compressed struts play a primordial role in the behavior and determination of the bearing capacity of the pile caps.

3. Deep pile caps strength evaluation

The sectional approach and the STM are Mostly proposed to evaluate the bearing capacity of four pile caps piles. The first method, known as sectional design, assumes that a pile cap acts like a reinforced concrete beam spanning two or more piles. The conventional beam theory is used to determine the sectional depth and amount of tension reinforcement, assuming that the plane section remains plane. The ACI code, for example, recommends designing pile caps using the same sectional approach used for footings supported on soil and two-way slabs directly.

The second approach uses a strut-and-tie model (STM). According to this approach, the complex flow of stresses in a pile cap can be idealized by the 3D- STM as space truss-like members of diagonal concrete struts and steel reinforcement ties connected at each node (Fig. 2). Furthermore, previous researchers (Adebar et al. [7], Adebar and Zhou [18], and Cavers and Fenton [19]) have confirmed that STM-based pile cap design is superior to the former approach. However, the most proposed strut-and-tie- models based on the geometric shape of the truss in pile cap design are fundamentally similar; the node location, and thus the resulting strut inclination θs^{3d}, do not always coincide (Fig. 2).

This section investigates the recent and most efficient STMs for calculating nominal strength.

Souza et al. [15] assumed that the four-pile cap could fail by shear

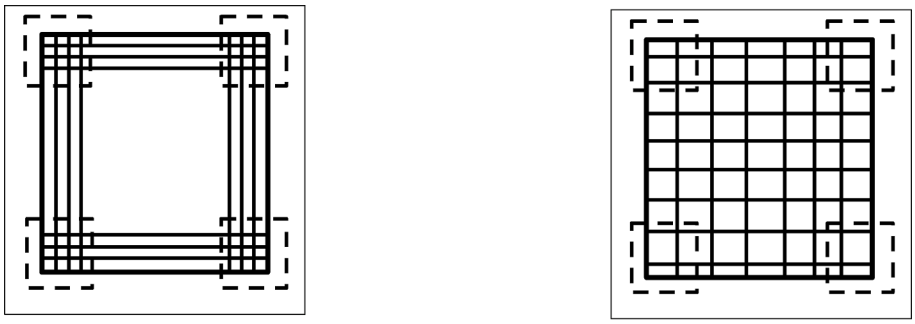

(a) Bunched square layouts (b) Grid pattern layouts

Fig. 1. Various layouts of main reinforcing Bars (four pile caps).

Table 1
Sizing of the equivalent concrete-steel tie and the simplified equivalent struts corresponding to the pile cap BP-30–30-2 [8].

	P_{test} (kN)	f_c'(MPa)	d (mm)	c (mm)	(b) (mm)	a (mm)	A_S (mm2)	f_y(Mpa)	$P_{n,f}$(KN)	$P_{n,s}$(KN)	P_n(KN) (Equation (11))	$A_{Strut}(mm^2)$	$A_{Tie}(mm^2)$	$4750\sqrt{f_c'}$(MPa)	Elastic moduli of tie element (MPa)	P_{test}/P_{model}
BP-30–30-2 [8]	**907**	**28,5**	**250**	**300**	**800**	**100**	**567**	**405**	**909.708**	**760.88**	**760.88**	**14377.213**	**449.238**	**25358.06**	**200,000**	**1,19**

(strut splitting) or flexure, where a single criterion for predicting the failure load was determined. This simplification suggested a significant change in the inclination struts and, as a result, the forces generated by the truss system.

The bearing capacity was determined by:

$$P_n = Min\begin{cases} P_{n(shear)} \\ P_{n(flexure)} \end{cases}; P_{n(shear)} = 2.08cd\left(f_c'\right)^{\frac{2}{3}}; P_{n(flexure)} = 2.05\frac{4.A_s f_y.d}{l_e} \quad (1)$$

where: A_s is the total reinforcement in one direction; f_c' the compressive strength of the concrete cylinder; f_y the yield stress of reinforcement; c the width of Colum; d depth of reinforcement; l_e pile spacing; P_n the nominal strength at failure proposed by the authors.

Meléndez et al. [2] proposed a lower-bound strength function, which varies with θ_s^{3d}, defined by the three limit functions [$P_{nt,u}$, $P_{ns,1}$, $P_{ns,2}$] corresponding respectively to the three local failure Modes: yielding reinforcements, Crushing of the diagonal strut, and Splitting of the diagonal strut.

$$P_{nt,u} = 2\sqrt{2}tan\theta_s^{3d}A_s f_u \quad (2)$$

$$P_{ns,1} = 18f_{cp}\left(\frac{d}{\sqrt{2}\,tan\theta_s^{3d}} - a\right)^2 sin^2\theta_s^{3d} \quad (3)$$

$$P_{ns,2} = \frac{4\beta_p sin\theta_s^{3d}(d_p sin\theta_s^{3d} + 2C_b cos\theta_s^{3d})d_p f_{cp}}{0.8 + 170(\varepsilon_{tx} + \varepsilon_{ty} + \varepsilon_z - \varepsilon_s)} \quad (4)$$

where: θ_s^{3d} present the 3-D strut angle; f_u steel ultimate; f_{cp} the equivalent plastic strength of concrete;β_p area factor of projection of pile perpendicular to strut direction; ε_{tx} and ε_{ty} reinforcement strain in x- and y-direction; ε_z the average concrete strain in the z-direction;ε_s an average compressive strain of concrete strut.

As a result, the maximum (peak) value of the lower-bound strength function P_n defined by equation (5) will be the best estimate of the pile cap strength, whichever gives the lowest load.

$$P_n = Min(P_{nt,u}, P_{ns,1}, P_{nt,u}) \quad (5)$$

The shear strength P_s is represented by the intersection of the functions of $P_{ns,1}$ and $P_{ns,2}$, whereas the flexural strength P_f is represented by the intersection of functions $P_{ns,1}$ and $P_{nt,u}$.

However, uncertainty in strength predictions of pile caps is observed following the results (COV = 13.8% with minimum (P_{test}/P_{model}) = 0.73 for Souza et al. [15] and COV = 11.1% with minimum (P_{test}/P_{model}) = 0.83 for Meléndez et al. [2]). Moreover, the method proposed by Meléndez et al. [2] is considered too complex for practical design purposes.

The ACI 318–14 [20] uses the sectional approach and STM to design a pile cap. For the sectional method, the critical flexural section is located on the column's face, which is the longitudinal reinforcement determining the flexural strength. The shear strength is determined by the most restrictive condition considering one-way and two-way shear and governing by the cap depth and concrete strength.

The CRSI Handbook code [21] proposes to consider the upper limit of the shear strength corresponding to the case of two-way shear without any contribution of the reinforcements:

$$V_C = \frac{d}{a}\left(1 + \frac{d}{c}\right)\frac{1}{6}\sqrt{f_c'}b_0 d \le 2.67\sqrt{f_c'}b_0 d \quad (6)$$

where b_0 is the column perimeter; and f_c' is in MPa.

BOULIFA et al. [3] propose a sectional approach to predict the bearing capacity of four pile caps, considering the contributions of the concrete and the longitudinal reinforcements.

The bearing capacity of four pile caps, P_n, is twice that of the resulting shear in the vertical plane of symmetry (plan Y-Y'), F_3. (Fig. 3).

The vertical equilibrium of the vertical plane of symmetry of the pile

Table 2
Comparison of the ratios (experimental load on predicted load) of the proposed model with the predictions proposed by the three theoretical methods.

Specimens	P_{test} (kN)	f'_c(MPa)	a /d	d (mm)	cap size b (mm)	A_S (mm^2)	Steel grade (MPa)	Souza et al. [15]		CRSI Handbook code [21]	Meléndez et al. [2]	Proposed model		P_{test}/P_{Model}				Observed failure modes	Predicted failure modes
								P_n(KN) (shear)	P_n(KN) (flexion)	P_n(KN) two-way shear		$P_{n,S}$(KN) (shear)	$P_{n,fP}$(KN) (flexion)	(a)	(b)	(c)	(d)		
Suzuki et al. [8]																			
BP-20–1	519	21.3	0.8	150	900	567	413	719.22	533.39	203.89	436.13	412.29	468.26	0.97	2.55	1.19	1.26	f + s	s
BP-20–2	480	20.4	0.8	150	900	567	413	698.82	533.39	199.54	428.57	408.18	467.51	0.9	2.41	1.12	1.18	f + s	s
BPC-20–1	519	21.9	0.8	150	900	567	413	732.66	533.39	206.74	513.86	414.99	468.75	0.97	2.51	1.01	1.25	f + p	s
BPC-20–2	529	19.9	0.8	150	900	567	413	687.35	533.39	197.08	494.39	405.85	467.09	0.99	2.68	1.07	1.3	f + p	s
BP-25–1	735	22.6	0.6	200	900	709	413	997.59	889.3	414.86	644.74	630.76	770.42	0.83	1.77	1.14	1.17	s	s
BP-25–2	755	21.5	0.6	200	900	709	413	964.95	889.3	404.64	634.45	624.23	769.23	0.85	1.87	1.19	1.21	s	s
BPC-25–1	818	18.9	0.6	200	900	709	413	885.5	889.3	379.38	687.39	608.12	766.3	0.92	2.16	1.19	1.35	f + s	s
BPC-25–2	813	22	0.6	200	900	709	413	979.86	889.3	409.32	745.87	627.22	769.77	0.91	1.99	1.09	1.3	f + p	s
BP-20–30-1	485	29.1	0.67	150	800	425	405	885.53	423.43	285.98	480.2	393.91	418.53	1.15	1.7	1.01	1.23	f + s	s
BP-20–30-2	480	29.8	0.67	150	800	425	405	899.68	423.43	289.4	480	396.3	418.97	1.13	1.66	1	1.21	f + s	s
BPC-20–30-1	500	29.8	0.67	150	800	425	405	899.68	423.43	289.4	480.77	396.3	418.97	1.18	1.73	1.04	1.26	f	s
BPC-20–30-2	495	29.8	0.67	150	800	425	405	899.68	423.43	289.4	480.58	396.3	418.97	1.17	1.71	1.03	1.25	f	s
BP-30–30-1	916	27.3	0.4	250	800	567	405	1414.4	941.5	940.42	776.27	753.86	908.43	0.97	0.97	1.18	1.22	s	s
BP-30–30-2	907	28.5	0.4	250	800	567	405	1455.5	941.5	960.87	788.7	760.89	909.71	0.96	0.94	1.15	1.19	f + s	s
BPC-30–30-1	1039	28.9	0.4	250	800	567	405	1469.1	941.5	967.59	927.68	763.2	910.13	1.1	1.07	1.12	1.36	f + s	s
BPC-30–30-2	1029	30.9	0.4	250	800	567	405	1536.1	941.5	1000.5	952.78	774.51	912.19	1.09	1.03	1.08	1.33	f + s	s
BP-30–25-1	794	30.9	0.5	250	800	567	405	1280.1	941.5	727.64	728.44	688.4	742.26	0.84	1.09	1.09	1.15	f + s	s
BP-30–25-2	725	26.3	0.5	250	800	567	405	1149.7	941.5	671.3	677.57	661.77	737.41	0.77	1.08	1.07	1.1	s	s
BPC-30–25-1	853	29.1	0.5	250	800	567	405	1229.9	941.5	706.13	836.27	678.23	740.41	0.91	1.21	1.02	1.26	f + s	s
BPC-30–25-2	872	29.2	0.5	250	800	628.3	405	1232.7	1043.3	707.34	838.46	716.06	814.02	0.84	1.23	1.04	1.22	f	s
BDA-70–90-1	784	29.1	0.5	250	800	628.3	345	1229.9	888.76	706.13	768.63	658.94	702.33	0.88	1.11	1.02	1.19	f	s
BDA-70–90-2	755	30.2	0.5	250	800	628.3	345	1260.7	888.76	719.35	778.35	665.19	703.46	0.85	1.05	0.97	1.14	f	s
BDA-80–90-1	858	29.1	0.5	250	950	628.3	345	1229.9	888.76	706.13	772.97	721.52	713.71	0.97	1.22	1.11	1.2	f	f
BDA-80–90-2	853	29.3	0.5	250	950	628.3	345	1235.5	888.76	708.55	775.45	722.88	713.95	0.96	1.2	1.1	1.19	f	f
BDA-90–90-1	853	29.5	0.5	250	900	628.3	345	1241.2	888.76	710.97	775.45	703.23	710.38	0.96	1.2	1.1	1.21	f	s
BDA-90–90-2	921	31.5	0.5	250	900	628.3	345	1296.6	888.76	734.67	780.51	715.84	712.67	1.04	1.25	1.18	1.29	f	f
BDA-100–90-1	911	29.7	0.5	250	950	628.3	345	1246.8	888.76	713.37	778.63	725.59	714.44	1.03	1.28	1.17	1.28	f	f

(*continued on next page*)

Table 2 (*continued*)

Specimens	P_{test} (kN)	$f_c^{'}$(MPa)	*a* /d	d (mm)	cap size b (mm)	A_S (mm^2)	Steel grade (MPa)	Souza et al. [15]		CRSI Handbook code [21]	Meléndez et al. [2]	Proposed model		P_{test}/P_{Model}				Observed failure modes	Predicted failure modes
								P_n(KN) (shear)	P_n(KN) (flexion)	P_n(KN) two-way shear		$P_{n,\ S}$(KN) (shear)	$P_{n,\ fP}$(KN) (flexion)	(a)	(b)	(c)	(d)		
BDA-100–90-2	931	31.3	0.5	250	950	628.3	345	1291.1	888.76	732.34	782.35	736.23	716.38	1.05	1.27	1.19	1.3	f	f
Clarke [6]																			
A1	1110	26.6	0.49	405	950	785	410	1501.3	1781.4	1339.9	1000	1102.7	1076.2	0.74	0.83	1.11	1.03	s	f
A2	1420	34	0.49	405	950	785	410	1768.2	1781.4	1514.9	1314.8	1182.9	1090.8	0.8	0.94	1.08	1.3	s	f
A4	1230	26.7	0.49	405	950	785	410	1505.1	1781.4	1342.4	1000	1103.9	1076.4	0.82	0.92	1.23	1.14	s	f
A5	1400	33.2	0.49	405	950	785	410	1740.4	1781.4	1496.9	1320.8	1174.7	1089.3	0.8	0.94	1.06	1.29	s	f
A7	1640	30.2	0.49	405	950	785	410	1633.9	1781.4	1427.7	1261.5	1142.9	1083.5	1	1.15	1.3	1.51	s	f
A8	1510	34	0.49	405	950	785	410	1768.2	1781.4	1514.9	1313	1182.9	1090.8	0.85	1	1.15	1.38	s	f
A9	1450	33.2	0.49	405	950	785	410	1740.4	1781.4	1496.9	1124	1174.7	1089.3	0.83	0.97	1.29	1.33	s	f
A10	1520	23.5	0.49	405	950	785	410	1382.3	1781.4	1259.4	1085.7	1065.8	1069.5	1.1	1.21	1.4	1.43	s	s
A11	1640	22.5	0.49	405	950	785	410	1342.8	1781.4	1232.3	1058.1	1053.4	1067.2	1.22	1.33	1.55	1.56	f	s
A12	1640	31.6	0.49	405	950	785	410	1684	1781.4	1460.4	1281.3	1157.9	1086.2	0.97	1.12	1.28	1.51	f	f
B1	2080	33.4	0.25	405	750	628	410	1747.3	2137.7	3002.9	1664	1325.2	1642.1	1.19	0.69	1.25	1.57	s	s
B2	1900	30.8	0.25	405	750	785	410	1655.4	2672.2	2883.6	*	1499.1	2024	1.15	0.66	*	1.27	s	s
B3	1770	43.7	0.25	405	750	471	410	2090.3	1603.3	3434.8	1393.7	1207.8	1270.4	1.1	0.52	1.27	1.47	f	s
Suzuki and Otsuki [11]																			
BPL-35–30-1	960	24.1	0.34	290	800	642	353	1509.8	1077.8	1275.4	864.86	845.27	1036.7	0.89	0.75	1.11	1.14	s	s
BPL-35–30-2	941	25.6	0.34	290	800	642	353	1571.8	1077.8	1314.5	887.74	856.07	1038.7	0.87	0.72	1.06	1.1	s	s
BPB-35–30-1	1029	23.7	0.34	290	800	642	353	1493.1	1077.8	1264.8	989.42	842.33	1036.2	0.95	0.81	1.04	1.22	f + s	s
BPB-35–30-2	1103	23.5	0.34	290	800	642	353	1484.7	1077.8	1259.4	984.82	840.85	1035.9	1.02	0.88	1.12	1.31	f + s	s
BPH-35–30-1	980	31.5	0.34	290	800	642	353	1804.9	1077.8	1458.1	980	895.75	1045.9	0.91	0.67	1	1.09	s	s
BPH-35–30-2	1088	32.7	0.34	290	800	642	353	1850.5	1077.8	1485.7	998.17	903.35	1047.3	1.01	0.73	1.09	1.2	f + s	s
BPL-35–25-1	902	27.1	0.43	290	800	642	353	1360.5	1077.8	990.29	827.52	767.97	846.08	0.84	0.91	1.09	1.17	f + s	s
BPL-35–25-2	872	25.6	0.43	290	800	642	353	1309.9	1077.8	962.49	807.41	757.49	844.17	0.81	0.91	1.08	1.15	s	s
BPB-35–25-1	911	23.2	0.43	290	800	642	353	1226.7	1077.8	916.27	893.14	740.04	841	0.85	0.99	1.02	1.23	f + s	s
BPB-35–25-2	921	23.7	0.43	290	800	642	353	1244.2	1077.8	926.09	902.94	743.75	841.67	0.85	0.99	1.02	1.24	f + s	s
BPH-35–25-1	882	36.6	0.43	290	800	642	353	1662.3	1077.8	1150.9	938.3	828.55	857.09	0.82	0.77	0.94	1.06	s	s
BPH-35–25-2	951	37.9	0.43	290	800	642	353	1701.5	1077.8	1171.1	960.61	836.2	858.48	0.88	0.81	0.99	1.14	s	s
BPL-35–20-1	755	22.5	0.52	290	800	642	353	961.49	1077.8	682.32	692.66	669.07	710.35	0.79	1.11	1.09	1.13	s	s
BPL-35–20-2	735	21.5	0.52	290	800	642	353	932.79	1077.8	666.99	680.56	661.41	708.96	0.79	1.1	1.08	1.11	s	s
BPB-35–20-1	755	20.4	0.52	290	800	642	353	900.7	1077.8	649.7	762.63	652.79	707.39	0.84	1.16	0.99	1.16	f + p	s
BPB-35–20-2	804	20.2	0.52	290	800	642	353	894.8	1077.8	646.51	758.49	651.2	707.1	0.9	1.24	1.06	1.23	f + s	s

(*continued on next page*)

Table 2 (*continued*)

Specimens	P_{test} (kN)	$f_c^{'}$(MPa)	*a* /d	d (mm)	cap size b (mm)	A_S (mm^2)	Steel grade (MPa)	Souza et al. [15]		CRSI Handbook code [21]	Meléndez et al. [2]	Proposed model		P_{test}/P_{Model}				Observed failure modes	Predicted failure modes
								P_n(KN) (shear)	P_n(KN) (flexion)	P_n(KN) two-way shear		$P_{n,\ S}$(KN) (shear)	$P_{n,\ fP}$(KN) (flexion)	(a)	(b)	(c)	(d)		
BPH-35–20-1	813	31.4	0.52	290	800	642	353	1200.7	1077.8	806.05	797.06	730.8	721.58	0.75	1.01	1.02	1.13	s	f
BPH-35–20-2	794	30.8	0.52	290	800	642	353	1185.4	1077.8	798.32	794	726.94	720.88	0.74	0.99	1	1.1	s	f
Suzuki et al. [10]																			
BDA-20–25-70–1	294	26.1	0.67	150	700	284	358	686.31	277.9	240.75	294	280.34	255.89	1.06	1.22	1	1.15	f	f
BDA-20–25-70–2	304	26.1	0.67	150	700	284	358	686.31	277.9	240.75	295.15	280.34	255.89	1.09	1.26	1.03	1.19	f	f
BDA-20–25-80–1	304	25.4	0.67	150	800	284	358	673.99	277.9	237.5	292.31	301.49	259.73	1.09	1.28	1.04	1.17	f	f
BDA-20–25-80–2	304	25.4	0.67	150	800	284	358	673.99	277.9	237.5	292.31	301.49	259.73	1.09	1.28	1.04	1.17	f	f
BDA-20–25-90–1	333	25.8	0.67	150	900	284	358	681.04	277.9	239.36	294.69	326.52	264.28	1.2	1.39	1.13	1.26	f	f
BDA-20–25-90–2	333	25.8	0.67	150	900	284	358	681.04	277.9	239.36	294.69	326.52	264.28	1.2	1.39	1.13	1.26	f	f
BDA-30–20-70–1	534	25.2	0.5	250	700	425	358	893.92	693.13	591.4	593.33	500.01	499.78	0.77	0.9	0.9	1.07	f	f
BDA-30–20-70–2	549	24.6	0.5	250	700	425	358	879.68	693.13	584.32	590.32	496.75	499.19	0.79	0.94	0.93	1.11	f + s	s
BDA-30–20-80–1	568	25.2	0.5	250	800	425	358	893.92	693.13	591.4	591.67	538.84	506.84	0.82	0.96	0.96	1.12	f	f
BDA-30–20-80–2	564	26.6	0.5	250	800	425	358	926.73	693.13	607.61	600	547.35	508.39	0.81	0.93	0.94	1.11	f	f
BDA-30–20-90–1	583	26	0.5	250	900	425	358	912.74	693.13	600.71	594.9	583.16	514.9	0.84	0.97	0.98	1.13	f	f
BDA-30–20-90–2	588	26.1	0.5	250	900	425	358	915.08	693.13	601.87	593.94	583.85	515.02	0.85	0.98	0.99	1.14	f	f
BDA-30–25-70–1	662	28.8	0.4	250	700	425	383	1221.4	741.53	878.1	727.47	595.75	655.09	0.89	0.75	0.91	1.11	f + s	s
BDA-30–25-70–2	676	26.5	0.4	250	700	425	383	1155.5	741.53	842.31	711.58	583.91	652.94	0.91	0.8	0.95	1.16	f + s	s
BDA-30–25-80–1	696	29.4	0.4	250	800	425	383	1238.3	741.53	887.2	732.63	640.7	663.27	0.94	0.78	0.95	1.09	f + s	s

(*continued on next page*)

Table 2 (*continued*)

Specimens	P_{test} (kN)	$f_c^{'}$(MPa)	*a* /d	d (mm)	cap size b (mm)	A_S (mm^2)	Steel grade (MPa)	Souza et al. [15]		CRSI Handbook code [21]	Meléndez et al. [2]	Proposed model		P_{test}/P_{Model}				Observed failure modes	Predicted failure modes
								P_n(KN) (shear)	P_n(KN) (flexion)	P_n(KN) two-way shear		$P_{n,S}$(KN) (shear)	$P_{n,fP}$(KN) (flexion)	(a)	(b)	(c)	(d)		
BDA-30–25-80–2	725	27.8	0.4	250	800	425	383	1193	741.53	862.72	725	631.44	661.58	0.98	0.84	1	1.15	f + s	s
BDA-30–25-90–1	764	29	0.4	250	900	425	383	1227.1	741.53	881.15	727.62	680.06	670.42	1.03	0.87	1.05	1.14	f + s	f
BDA-30–25-90–2	764	26.8	0.4	250	900	425	383	1164.2	741.53	847.06	720.75	665.56	667.79	1.03	0.9	1.06	1.15	f	s
BDA-30–30-70–1	769	26.8	0.3	250	700	425	358	1397.1	693.13	1242.4	818.09	660.65	801.57	1.11	0.62	0.94	1.16	f + s	s
BDA-30–30-70–2	730	25.9	0.3	250	700	425	358	1365.6	693.13	1221.3	802.2	655.91	800.7	1.05	0.6	0.91	1.11	f + s	s
BDA-30–30-80–1	828	27.4	0.3	250	800	425	358	1417.8	693.13	1256.2	819.8	704.26	809.49	1.19	0.66	1.01	1.18	f + s	s
BDA-30–30-80–2	809	27.4	0.3	250	800	425	358	1417.8	693.13	1256.2	825.51	704.26	809.49	1.17	0.64	0.98	1.15	f + s	s
BDA-30–30-90–1	843	27.2	0.3	250	900	425	358	1410.9	693.13	1251.6	818.45	743.41	816.61	1.22	0.67	1.03	1.13	f + s	s
BDA-30–30-90–2	813	24.5	0.3	250	900	425	358	1315.9	693.13	1187.9	774.29	724.92	813.25	1.17	0.68	1.05	1.12	f + s	s
BDA-40–25-70–1	1019	25.9	0.29	350	700	567	358	1593.2	1294.6	1958.6	961.32	918.58	1121.6	0.79	0.52	1.06	1.11	s	s
BDA-40–25-70–2	1068	24.8	0.29	350	700	567	358	1547.8	1294.6	1916.5	945.13	910.3	1120.1	0.82	0.56	1.13	1.17	f + s	s
BDA-40–25-80–1	1117	26.5	0.29	350	800	567	358	1617.7	1294.6	1981.1	971.3	978.77	1132.5	0.86	0.56	1.15	1.14	f	s
BDA-40–25-80–2	1117	25.5	0.29	350	800	567	358	1576.8	1294.6	1943.4	954.7	970.27	1131	0.86	0.57	1.17	1.15	f + s	s
BDA-40–25-90–1	1176	25.7	0.29	350	900	567	358	1585	1294.6	1951	956.1	1026.9	1141.3	0.91	0.6	1.23	1.15	f	s
BDA-40–25-90–2	1181	26	0.29	350	900	567	358	1597.3	1294.6	1962.3	960.16	1029.8	1141.8	0.91	0.6	1.23	1.15	f	s
Suzuki et al. [9]																			
TDL1-1	392	30.9	0.58	300	900	285.2	356	1536.1	416.28	823.28	395.96	594.87	342.02	0.94	0.48	0.99	1.15	f	f
TDL1-2	392	28.2	0.58	300	900	285.2	356	1445.3	416.28	786.48	395.96	574.12	338.25	0.94	0.5	0.99	1.16	f	f
TDL2-1	519	28.6	0.58	300	900	428	356	1458.9	624.71	792.04	570.33	642.62	467.8	0.83	0.66	0.91	1.11	f	f
TDL2-2	472	28.8	0.58	300	900	428	356	1465.7	624.71	794.81	568.67	644.18	468.08	0.76	0.59	0.83	1.01	f	f

(*continued on next page*)

Table 2 (*continued*)

Specimens	P_{test} (kN)	f'_c(MPa)	a /d	d (mm)	cap size b (mm)	A_S (mm^2)	Steel grade (MPa)	Souza et al. [15]		CRSI Handbook code [21]	Meléndez et al. [2]	Proposed model		P_{test}/P_{Model}				Observed failure modes	Predicted failure modes
								P_n(KN) (shear)	P_n(KN) (flexion)	P_n(KN) two-way shear		$P_{n,S}$(KN) (shear)	$P_{n,fP}$(KN) (flexion)	(a)	(b)	(c)	(d)		
TDL3-1	608	29.6	0.58	300	900	570	356	1492.7	831.97	805.77	653.76	715.36	597.47	0.73	0.75	0.93	1.02	f	f
TDL3-2	627	29.3	0.58	300	900	570	356	1482.6	831.97	801.68	653.13	713.05	597.05	0.75	0.78	0.96	1.05	f	f
TDS1-1	921	25.6	0.33	300	900	428	356	1355	832.95	1311.4	800.87	765.47	753.36	1.11	0.7	1.15	1.22	f	f
TDS1-2	833	27	0.33	300	900	428	356	1404	832.95	1346.7	816.67	776.87	755.43	1	0.62	1.02	1.1	f	f
TDS2-1	1005	27.2	0.33	300	900	570	356	1410.9	1109.3	1351.7	897.32	892.22	980.17	0.91	0.74	1.12	1.13	f	s
TDS2-2	1054	27.3	0.33	300	900	570	356	1414.4	1109.3	1354.2	900.85	893.02	980.32	0.95	0.78	1.17	1.18	f	s
TDS3-1	1299	28	0.33	300	900	784	356	1438.5	1525.8	1371.5	1007	1070	1319.6	0.9	0.95	1.29	1.21	f + s	s
TDS3-2	1303	28.1	0.33	300	900	784	356	1441.9	1525.8	1373.9	1010.1	1070.8	1319.7	0.9	0.95	1.29	1.22	f + s	s
TDM1-1	490	27.5	0.5	250	900	285	383	1184.4	447.54	686.44	441.44	528.77	389.47	1.09	0.71	1.11	1.26	f	f
TDM1-2	461	26.3	0.5	250	900	285	383	1149.7	447.54	671.3	439.05	520.71	388	1.03	0.69	1.05	1.19	f	f
TDM2-1	657	29.6	0.5	250	900	428	383	1244	672.09	712.17	631.73	624.6	554.07	0.98	0.92	1.04	1.19	f	f
TDM2-2	657	27.6	0.5	250	900	428	383	1187.3	672.09	687.69	625.71	611.58	551.71	0.98	0.96	1.05	1.19	f	f
TDM3-1	1245	27	0.5	250	900	1270	370	1170	1926.6	680.17	876.76	1066.6	1456.7	1.06	1.83	1.42	1.17	s	s
TDM3-2	1210	28	0.5	250	900	1270	370	1198.7	1926.6	692.66	889.71	1073.2	1457.9	1.01	1.75	1.36	1.13	s	s
AVERAGE														**0.95**	**1.05**	**1.08**	**1.20**		
COEFFİCİENT OF VARİATİON														**13.8%**	**43.1%**	**11.1%**	**8.8%**		
MAXİMUM														**1.22**	**2.68**	**1.55**	**1.57**		
MİNİMUM														**0.73**	**0.48**	**0.83**	**1.01**		

Note: (a) STM Model proposed by Souza et al. [15]; (b) Sectional approach corresponding to the two-way shear by the CRSI Handbook code [21]; (c) STM Model proposed by Meléndez et al. [2]; (d) Proposed approach; * Test not presented by the authors [2]; s = Shear failure; f = Flexural failure; f + s = Flexure and shear failure; f + p = Flexure and punching shear failure.

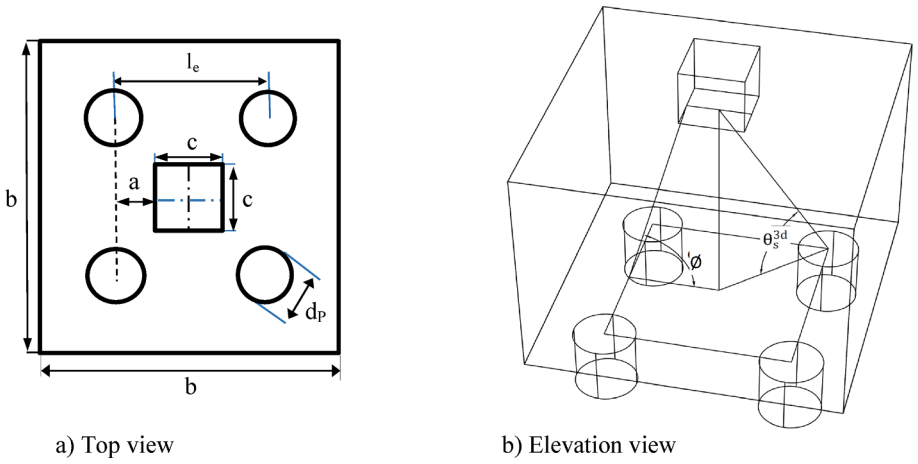

a) Top view b) Elevation view

Fig. 2. Strut –and –tie model and Key dimensions for four pile caps.

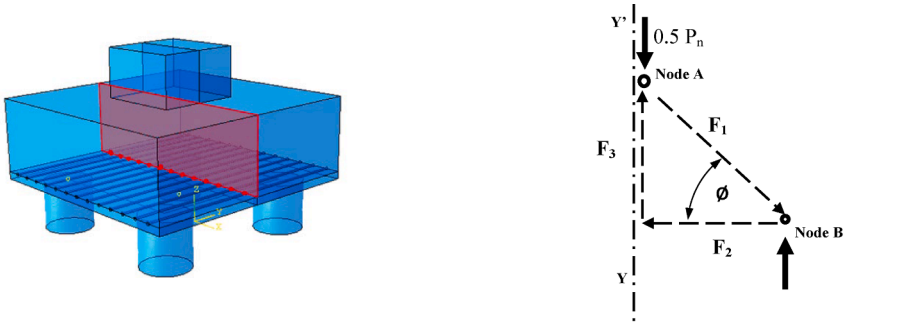

(a) Vertical plane of symmetry (3D view)

(b) Equivalent reaction forces at the nodal zones

Fig. 3. Equivalent load at the vertical plane of symmetry [3].

cap is given as.

$P_n = 2F_3$; $F_3 = F_2 tan\varnothing$ with.$F_2 = F_{2A} + F_{2B}$

$$F_{2A} = A_S\left(\frac{f_y}{2}\right);\ F_{2B} = b\left(\frac{a}{4}\right)\left(0.375\sqrt{f_c'}\right)$$

The predicted bearing capacity of four pile caps P_n is given by equation (7) below:

$$P_n = 2\left(A_S\left(\frac{f_y}{2}\right) + b\left(\frac{a}{4}\right)\left(0.375\sqrt{f_c'}\right)\right)\frac{d}{a} \tag{7}$$

where:

F_{2A} the contribution of the reinforcements; F_{2B} the contribution of the concrete;

A_S Represents the total reinforcement crossing the vertical plane of symmetry (regarding the considered direction).$b\left(\frac{a}{4}\right)$ represents the effective area of the concrete tie on the rectangular plane of symmetry (section surrounding the reinforcements);

P_n: Predicted bearing capacity of four pile caps; d Depth of reinforcement;

b Width of the vertical plane of symmetry; a: The distance from pile center-line to column edge measured parallel to pile cap side $a = 0.5(l_e\text{-}c)$;$\frac{a}{d}$: Shear span-to-depth ratio; f_c': Compressive strength of concrete cylinder; $\left(0.375\sqrt{f_c'}\right)$: The tensile strength of concrete; f_y Yield stress of reinforcement.

Compared to the experimental data, equation (7) obtains exciting results for the punching failure mode (COV = 5% with minimum P_{test}/P_n of 1.21). However, for all the failure modes, the model's efficiency decreases significantly (COV = 10.8% with minimum P_{test}/P_n equal to 0,861).

The section below aims to calibrate both predictions proposed by equation (7), concrete and reinforcements, where the new model's performance is more efficient in precision and safety for all experimental failure modes.

4. Proposed model

The current study, which is interested in developing a model, focuses on evaluating accurately the contribution of concrete and reinforcements corresponding to the mode of failure by shear or bending and taking into consideration the main parameter, which is the shear-span depth ratio. Based on the prediction of four pile caps proposed by BOULIFA et al. [3], equation (7) can be presented in the form below:

$$P_n = 2.[\alpha.A_S.f_y + \beta.b.a(0.375\sqrt{f_c'})].\frac{d}{a} \tag{8}$$

The contribution of the longitudinal reinforcements is.$F_{2A} = \alpha.A_S.f_y$

The contribution of the concrete (effective area of the concrete tie) is.$F_{2B} = \beta.b.a(0.375\sqrt{f_c'})$

α: The yielding reinforcements ratio varying to from 0 at 1.

β: The contribution of the concrete ratio varying from 0 at 1.

By analyzing the variability of the coefficient of variation (COV) of the (P_{test}/P_{model}) with α "or" β, the most effective ratios corresponding to the failure mode can be assessed.

The experimental data used for calibration of α and β correspond to the four-pile caps experimental results obtained by Clarke [6] Suzuki et al.[8–10,12] and Suzuki and Otsuki [11] for members with a shear span-depth ratio (a/d) ranging from 0.25 to 0.8 and uniform grid

(bunched or rectangular mesh) reinforcement layout. The classification of the experimental data according to the failure mode corresponds to 27 pile caps failing by shear, 43 pile caps failing by flexion, and 37 pile caps failing by the combined failed mode; flexion and shear or flexion and punching. For each experimental failure mode, the variability of the coefficient of variation ratio of the (P_{test}/P_{model}) (COV) is investigated as follows:

- -The value of β must be fixed, and the variation of (COV) as a function of α should be studied.
- In the same way, the value of α should be fixed, and the variation of (COV) as a function of β should be investigated.

Fig. 4 (a) and 4 (b) show that the reinforcement contribution to overall bearing capacities is most dominant for the cases of flexural failure pile caps. Still, the contribution of concrete is required to be considered. The lowest coefficients of variation correspond to $\alpha \geq 0.6$ and $\beta \leq 0.1$, and the variability of the coefficient of variation as a function of β displays a concavity between $\beta = 0$ and $\beta = 0.2$.

The interaction between the concrete and the reinforcements is crucial in determining the load-bearing capacity of four pile caps failing by shear or combined shear and flexure mode. For the case of pile caps failing by shear mode, the weakest (COV) corresponds to the almost equal contribution of concrete and reinforcements between 35% and 45% (Fig. 5). However, in the case of flexural-shear and flexural-punching failures, the yielding reinforcements increase while the contribution of the concrete decreases (the weakest value of (COV) corresponds to $\alpha = 0.5$ and $\beta = 0.25$; Fig. 6).

Fig. 7 shows the variability of the coefficient of variation for all the pile caps failed by shear or combined shear-bending. The minimum (COV) value equals 0.08, corresponding to a yielding ratio of 0.375 (37.5%) and a rapport contribution of the concrete equal to 0.4125 (41.25%).

Consequently, the prediction of the bearing capacity of pile caps that failed in the flexure mode is determined by the following equation:

$$P_{n,f} = 2.[(0.74).A_S.f_y + (0.075).b.a(0.375\sqrt{f_c'})].\frac{d}{a} \quad (9)$$

$\alpha = 0.74$ and $\beta = 0.075$.

Moreover, the proposed prediction for the cases of pile cap failed due to the shear and shear-flexion modes presented by the equation:

$$P_{n,S} = 2.[(0.375).A_S.f_y + (0.4125).b.a(0.375\sqrt{f_c'})].\frac{d}{a} \quad (10)$$

$\alpha = 0.375$ and $\beta = 0.4125$.

The proposed model considers that the bearing capacity of four pile caps equal to the lower-bound strength between the prediction of pile caps that fail due to flexion mode and pile caps that fail in the presence of shear mode as

$$P_n = Min\begin{cases} P_{n,f} \\ P_{n,S} \end{cases} \quad (11)$$

The proposed model agrees with the experimental results and demonstrates the effectiveness of the proposed α and β values corresponding to flexion or shear modes (pile caps failing with or without yielding steel).

However, it should be necessary to explain the physical significance of the different contributions of the two materials (concrete and steel) for each failure mode, as this is essential to justify this proposal.

5. Validation of the proposed approach using 2D -STM model

Strut-and-tie models are suitable for representing the stress field in pile cap foundations. Several analytical models for predicting the bearing capacity of pile caps based on 3D truss models have been proposed in scientific literature [4,7,14,15,18]. Most of these references focused on the proposal of different formulae to limit the concrete strength of the diagonal strut to evaluate the failure load accurately. The truss geometry received little consideration despite having an impact on the resulting strut forces, and these authors assumed a predefined truss geometry.

The present section concerned the verification of the proposed approach for determining the bearing capacity of four pile caps through the analogy of a 2D strut and tie model (triangular-shaped truss mechanism); the vertical load is evaluated based on the estimation of the tension in the tie element relative to the predicted failure load of pile cap (P_n) where the forces on the struts and tie elements are calculated by using the proposed analytical formulas ($P_{n,S}$ and $P_{n,f}$).

The Fig. 8 presents the 2D -STM geometry:

The sizing of struts and tie are givens using equations (9) and (10).

The compression force in the simplified equivalent concrete struts at failure is:

$$F_1 = \frac{P_{n,S}}{2sin\varnothing} = \frac{P_{n,S}.\sqrt{a^2+d^2}}{2d} \quad (12)$$

Which allowed the determination of the section of the simplified concrete struts element:. $A_{Stut} = F_1/f_c'$ where: $P_{n,S}$ is the predicted load for the case of shear failure.

The tension force in the equivalent concrete-steel tie at failure is:

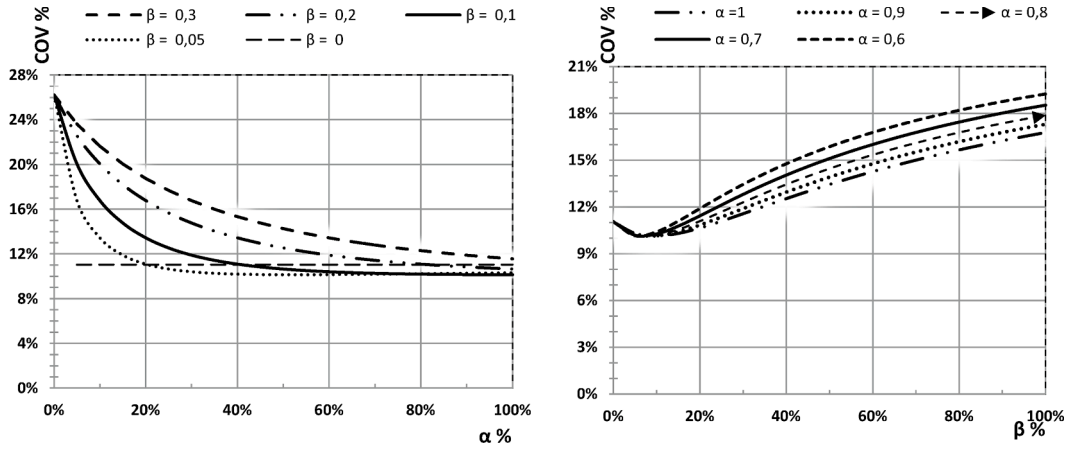

(a) Variation of (COV) as a function of α (b) Variation of (COV) as a function of β

Fig. 4. Variability of (COV) as a function of α and β for the case of 43 pile caps failing in flexion mode.

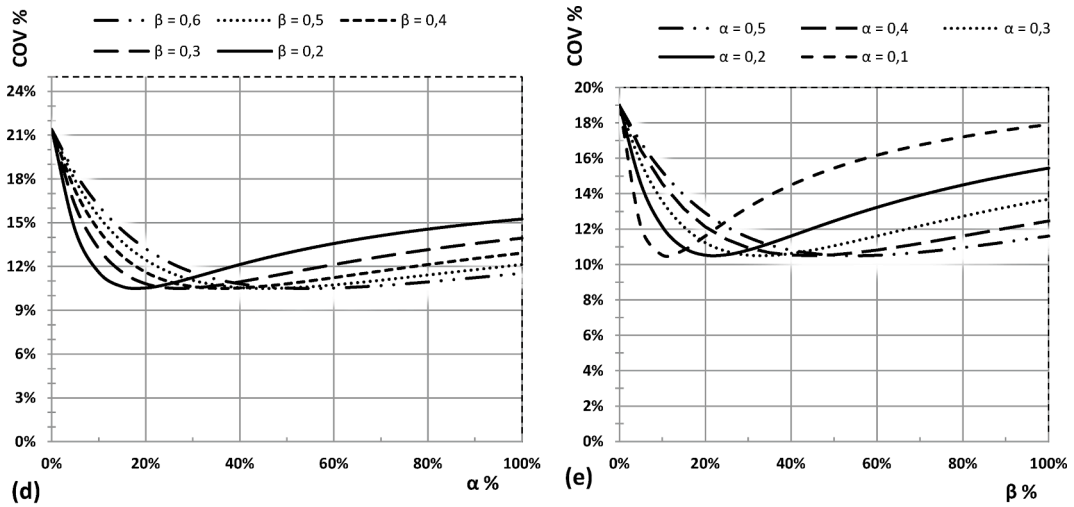

(a) Variation of (COV) as a function of α (b) Variation of (COV) as a function of β

Fig. 5. Variability of (COV) as a function of α and β for the case of 27 pile caps failing in shear mode.

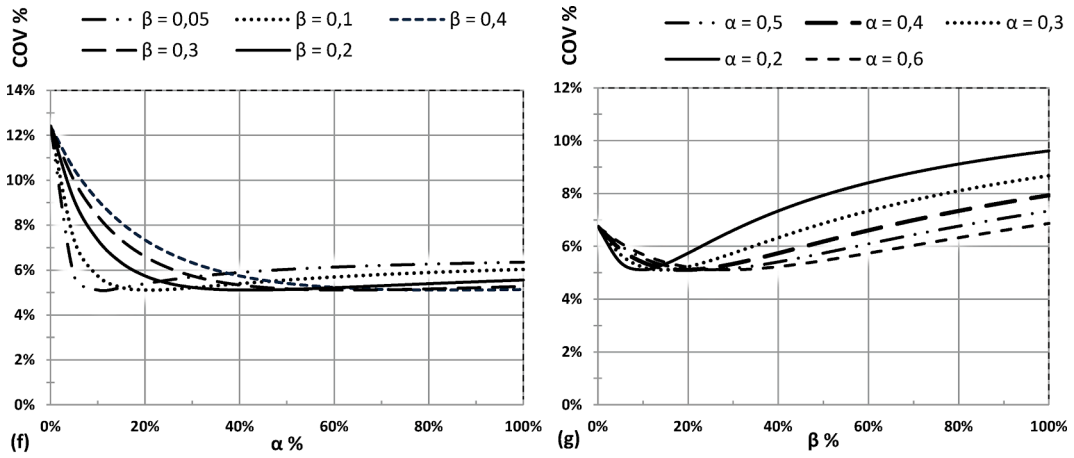

(a)Variation of (COV) as a function of α (b) Variation of (COV) as a function of β

Fig. 6. Variability of (COV) as a function of α and β for the case of 37 pile caps failing in combined flexion–shear modes.

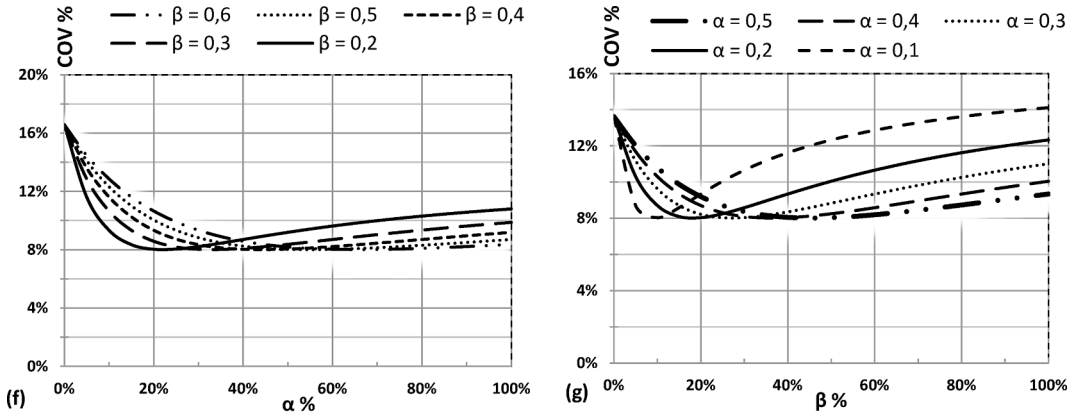

(a)Variation of (COV) as a function of α (b) Variation of (COV) as a function of β

Fig. 7. Variability of (COV) as a function of α and β for the case of 64 pile caps failed by shear alone (27) and combined shear-flexion modes (37).

$$F_2 = \frac{P_{n,f}}{2tan\emptyset} = \frac{P_{n,f}.a}{2d} \quad (13)$$

The section of the tie element is: $A_{Tie} = F_2/f_y$where: $P_{n,f}$ is the predicted load for the case of the flexure failure.

The assumptions in the proposed 2D-STM are further verified through FE analysis obtained with the "ABAQUS CAE" Software. For

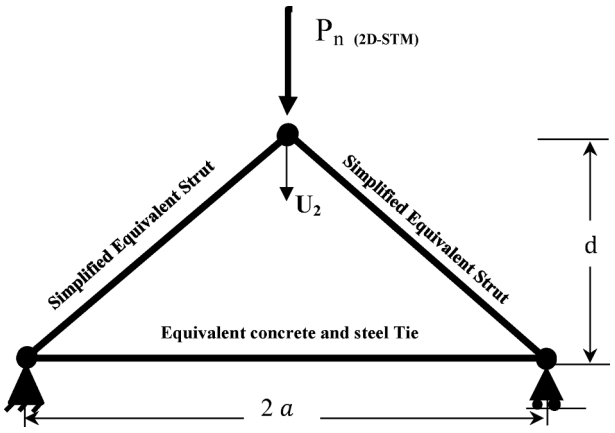

Fig. 8. 2D-STM and truss geometry.

modeling detail of pile cap BP-30–30-2 [8], the elastic moduli adopted for steel tie and concrete strut were 200000 MPa and $4750\sqrt{f_c'}$ (MPa) [20].

The compressive concrete strut element was modeled using the concrete damaged plasticity model [22]; the behavior of the concrete in the compression is parabolic, with the compressive strength of the concrete cylinder being f_c' occurs at strains between 0.002 and 0.0025, as defined in the *fib* Model Code 2010 [23]. The reinforcement steel's behavior was considered an elastic–plastic model with a yield plateau varying from strains 0.002 to 0.01 [17]. To validate the proposed approach, the finite element simulations of 2D -STM was used to predict the behavior and bearing capacity of the specimen BP-30–30-2 [8] as an example case for comparison with 3D-STM proposed by Meléndez et al. [2] and the measured load–deflection curve. The table below presents the sizing of the equivalent concrete-steel tie and the simplified struts for the selected pile cap.

Fig. 9 shows the behavior obtained using the simulation of the equivalent truss (2D-STM) of the pile caps BP-30–30-2 [8] in terms of the load-vertical displacement curves of the top node.

The comparison of the load–displacement curve obtained from FE simulation of the equivalent truss, where the loads' values are multiplied by the ratio (P_{Test} /P_n = 1.19), with the measured load–deflection curve for the pile cap BP-30–30-2 [8,2] and the 3D- STM proposed by Meléndez et al. [2] prove that:

- The load–displacement curve obtained by the simplified 2D-STM's FE simulation, based on the proposed analytical formula, very acceptably converged with the four-pile cap behavior of the experimental specimen BP 30–30-2[8].
- The 3D-STM proposed by Meléndez et al. [2] more accurately anticipates the behavior of the specimen in comparison to the proposed 2D-STM, which did not accurately predict the nonlinearity of the load–deflection response.
- Regarding the experimental failure mode, the proposed model agreed with the experimental observations and the 3D-STM presented by Meléndez et al. [2] (shear failure mode).

However, to demonstrate that the proposed model can accurately depict the impact of various circumstances on the element response, a significant number of specimens must often be considered.

The section of the following study concerns the application of the proposed model's equation (Eq. (11)) to all experimental failure modes. The four-pile cap results obtained by Clarke[6], Suzuki et al.[8–10,12] and Suzuki and Otsuki [11]; were used for a comparative analysis based on STM proposed by Souza et al. [15], Meléndez et al. [2], and CRSI Handbook code [21]. The only pile caps studied were those with reinforcement bunched over the piles, distributed in a uniform grid, or both layouts.

6. Comparisons with test results and discussion

One hundred seven pile cap tests reported in the literature [8–12] (Table 2) were used to validate the relations given by the proposed model. In the plan, no shear reinforcement, and all specimens had been loaded at a centered square column. The proposed approach assumes

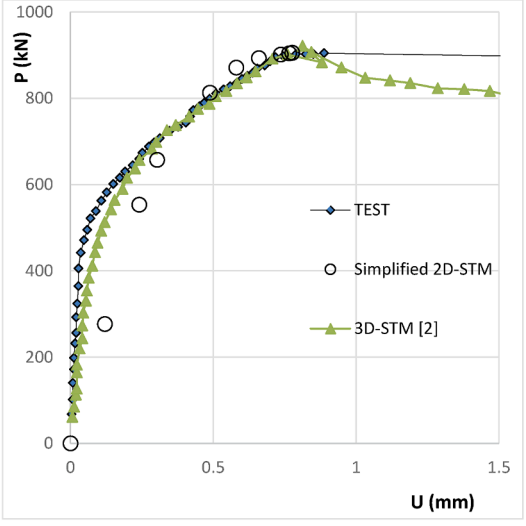

(a) load-displacement curves for the pile cap BP-30-30-2 [8]

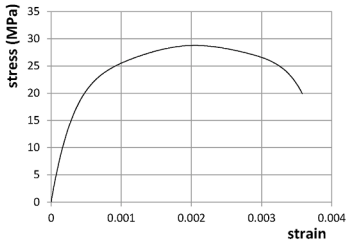

(b) stress-strain response of the concrete strut in compression (used for the simulation of the simplified 2D-STM)

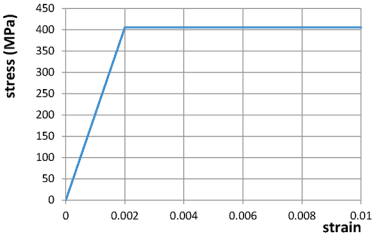

(c) Elastic-plastic behavior of equivalent concrete-steel tie in tension (used to simulate the simplified 2D-STM)

Fig. 9. Comparison of the load–displacement curve obtained from FE simulation of the simplified 2D-STM based on the proposed analytical formula (P_n), the loads' values are multiplied by the ratio (Ptest /Pn = 1.19), with the 3D- STM proposed by Meléndez et al. [2] and the measured load–deflection curve for the pile cap BP-30–30-2 [8].

that the steel reinforcement is identical in both orthogonal cap directions. The comparison concerns the STM Model proposed by Souza et al. [15], Meléndez et al. [2], and the sectional approach corresponding to the case of the two-way shear proposed by the CRSI Handbook code [21].

Table 2 shows the calculation results regarding the ratio of experimental load to predicted load for the proposed model and the results from the sectional approach and the STM Models [15, 2, and 21].

The provisions for a shear design using stress limits from the two-way shear of the CRSI Handbook [21] overestimated the measured strength predictions for many pile caps (Fig. 10 (b)).

The results of predictions using the approach developed by Melendez et al. [2] (Fig. 10(c)) have a relatively present low scatter (COV = 11%). Still, the proposed model underestimated 24 pile caps out of 107 specimens ($P_{test}/P_{model} < 0$) with a minimum value of (P_{test}/P_{model}) equal to 0.83.

Predictions by Souza et al. [15] (Fig. 10(a)) have a higher scatter (COV = 13.8%) compared to the STM model proposed by Meléndez et al. [2]. with an average (P test /P model) ratio of 0.95. the formulas proposed by Souza et al. [15] and the sectional approach of CRSI Handbook code [21] to predict shear design do not accurately capture the influence of pile cap depth on shear strength; both methods overestimate the shear strength considering depth altogether in the contributes to resisting transverse tensile stresses. Meléndez et al. [2]. on the other hand, demonstrated that the internal flow of forces in the pile cap exhibits stress concentration at specific areas of the section, as clarified by FE analysis.

The proposed model considers the correct depth of concrete (section surrounding the reinforcements). The proposed approach corresponds to the lowest COV (8.8 %) with an average value slightly above 1.2 (Fig. 10 (d)). The consideration of the concrete contribution in the flexure failure mode and the yielding of the reinforcement in the shear failure mode permit to decrease of the gap between the maximum and minimum value of (P_{test}/P_{n}) in a significant way with a minimum value equal to one.

A specific analysis of each failure mode has been qualified as initial observations can highlight the strengths and weaknesses of the proposed model corresponding to each failure mode.

Regarding Fig. 11. it is observed that the proposed model provides conservative values for the three failure modes (all the experimental data tests) (Fig. 11 a), followed by the model proposed by Meléndez et al. [2]. The CRSI Handbook code [21] shows the least secure results. Considering the accuracy of the predictions in terms of coefficient of variation (Fig. 11 b), the proposed model shows more accurate results for the two failure modes; bending alone and combined bending-shear. In comparison, it shows very close results to the model proposed by Meléndez et al. [2] for the case of shear-alone failure (COV = 11.4 for the prediction proposed by Meléndez et al. [2] and COV = 11.5 for the proposed model).

The model proposed in this work predicts the failure mode according to two evaluations of the load-bearing capacity: flexure failure $P_{n,f}$ or shear failure $P_{n,S}$. The results correspond to 68 specimens that failed by shear or combined shear-flexion and 39 by flexion, where 83 pile caps are correctly predicted (77.75%).

To conclude, the proposed model obtained a coefficient of variation concerning all the observations of (P_{test}/P_{model}) was found equal to 8.8%; This is a very appreciable and acceptable value compared to those found by the prediction of diagonal strut proposed by STM of ACI 318–14[20] (31%); Miguel-Tortola et al.[13] (13%).

7. Conclusion

The proposed approach for predicting the bearing capacity of four pile caps is based on evaluating the analytical failure loads by flexure or shear, considering both materials concrete and steel. The simple bilinear form of the analytical prediction equation allows for the determination

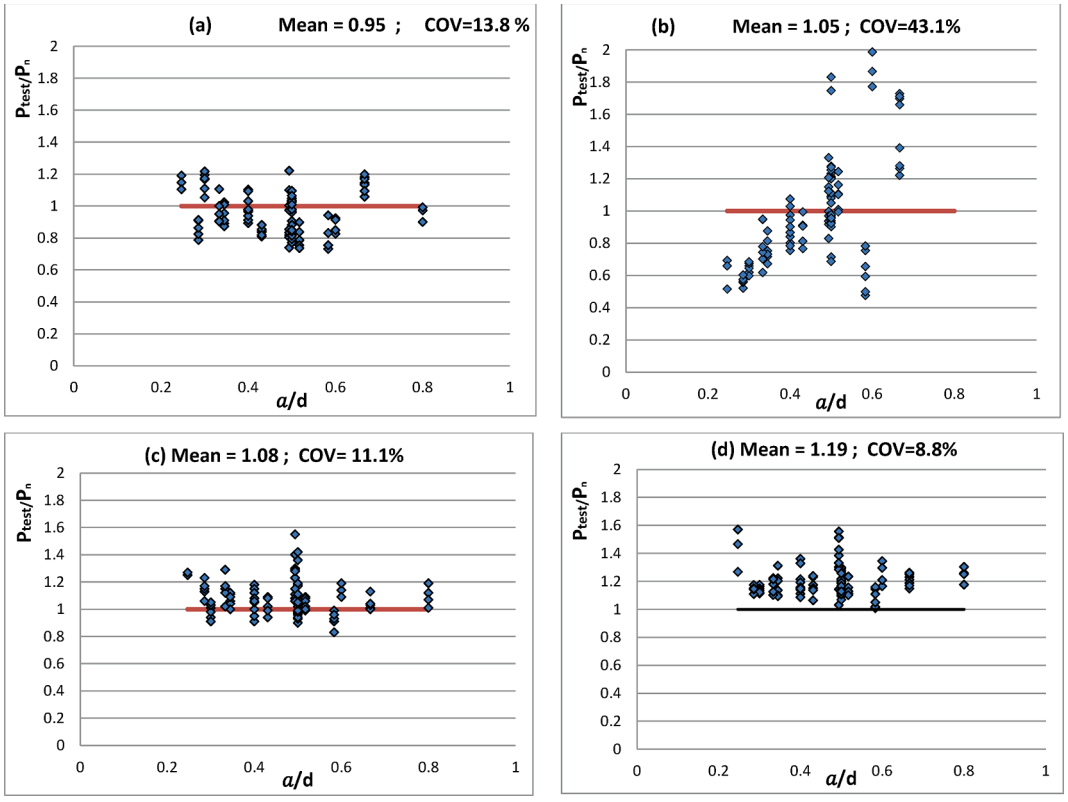

Fig. 10. Ratio (P_{test}/P_{model}) for 107 pile caps [8–12] based on results obtained by:: (a) STM Model proposed by Souza et al. [15]; (b) Sectional approach corresponding to the two-way shear by the CRSI Handbook code [21]; (c) STM Model proposed by Meléndez et al. [2]; (d) Proposed approach.

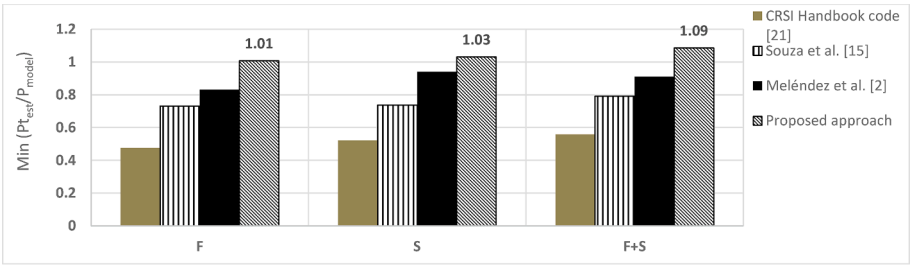

a) Minimum ratio of measured to predicted strengths

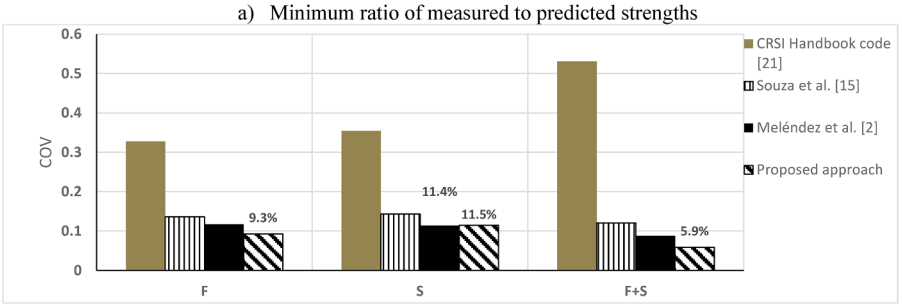

b) Coefficient of variation of the ratio of measured to predicted strengths

Fig. 11. Comparative presentation of statistical results of the proposed model with predictions proposed by three theoretical methods according to the different modes of failure observed; **s** *is a shear failure;* **F** *is a flexural failure;* **F + s** *is flexure and shear failure.*

of the combinations (α and β) corresponding to the lowest coefficient of variation.

The forces distribution between the concrete and the reinforcement is a critical parameter for predicting the bearing capacity of such structures. For flexure failure, the tension in the reinforcement is equivalent to the yielding of 0.74·As of reinforcement, and for shear failure is 0.375·As. The cross-section area of concrete in tension is 0.075·a·b for flexure failure and 0.4125·a·b for shear failure.

The comparison of the observed behavior of the BP-30–30-2 specimen [8] with the load–deflection curve obtained by the numerical simulation of the equivalent 2D-STM based on the analytical approach and the 3D-STM curve proposed by Melendez et al. [2], proves uncertainties about the behavior of these elements for the case of the proposed 2D simulation.

The proposed equation was the most accurate in predicting the bearing capacity of four pile caps; comparing the expected load by the current approach and those obtained from the literature with the experimental results database looks encouraging, and the results were in good agreement with the predicted ones. They were on the side of safety for all experimental results presented in this paper ($(P_{test}/P_n) \geq 1$, with an average ratio of 1,2.

Author Statement.

All authors certify that they have participated sufficiently in the work to take public responsibility for the content, including participation in the manuscript's concept, design, analysis, and writing. Furthermore, each author certifies that this or similar material has not been submitted to or published in any other publication.

CRediT authorship contribution statement

Ridha Boulifa: Conceptualization, Data curation, Software, Writing – original draft, Writing – review & editing. **Kamel Goudjil:** Writing – original draft, Writing – review & editing. **Mohamed Laid Samai:** Supervision, Methodology.

Declaration of Competing Interest

The authors declare that they have no known competing financial interests or personal relationships that could have appeared to influence the work reported in this paper.

Data availability

Data will be made available on request.

ACKNOWLEDGMENTS

The authors wish to thank the Algerian Ministry of Higher Education and Scientific Research for funding Project: A01L02UN410120210001.

Appendix A. . List of symbols

A_s	the total reinforcement in the considered direction (regarding one direction).
A_{Stut}	the section of the simplified concrete struts element
A_{Tie}	The section of the tie element
a	the distance from the pile center-line to the column edge measured parallel to the pile cap side;
b_0	is the column perimeter
C	width of Colum
d	depth of reinforcement
d_p	pile diameter/side
F_1	The compression force in the simplified equivalent concrete struts at failure
F_2	The tension force in the equivalent concrete and steel tie at failure
F_3	half of the shear force at the vertical plane of symmetry

(*continued on next page*)

(*continued*)

A_s	the total reinforcement in the considered direction (regarding one direction).
$f_c^{'}$	compressive strength of the concrete cylinder
f_y	yield stress of reinforcement
f_{cp}	equivalent plastic strength of concrete
f_u	steel ultimate
h	pile cap depth
l_e	pile spacing
P_{Model}	the nominal strength at failure proposed by different theoretical models
P_n	the nominal strength at failure proposed by the authors
P_{test}	measured capacity of test structure at failure
$P_{n\ (2D\text{-}STM)}$	vertical load obtained by the FE simulation of the simplified 2D-STM
$P_{nt.u}$.$P_{ns.1}$.$P_{ns.2}$	present the limit functions corresponding respectively to the local failure Modes (yielding reinforcements), (Crushing of the diagonal strut), and (Splitting of the diagonal strut).
COV	coefficients of variation
STM	Strut-and-Tie Model
Ø	present the 2-D strut angle
α	The yielding reinforcements ratio varying to from 0 at 1
β	The contribution of the concrete ratio varies from 0 at 1
β_p	area factor of projection of pile perpendicular to strut direction
θ_s^{3d}	3-D strut angle
ε_s	the average compressive strain of concrete strut
ε_{tx} ε_{ty}	reinforcement strain in x- and y-direction
ε_z	average concrete strain in the z-direction

References

[1] Muttoni A. Punching Shear Strength of Reinforced Concrete Slabs without Transverse Reinforcement. ACI Struct J 2008;105(4):440–50. https://doi.org/10.14359/19858.

[2] Meléndez C, Sagaseta J, Miguel Sosa PF, Pallarés RL. Refined Three-Dimensional Strut-and-Tie Model for Analysis and Design of Four- Pile Caps. ACI Struct J Jul 2019;116(04):15–29. https://doi.org/10.14359/51714485.

[3] Ridha Boulifa, Mohamed Laïd Samai, Mohamed Tayeb Benhassine, and Abdelhadi Tekkouk. Predicting Strength Capacity of Three-Dimensional Concrete Struts in Pile Caps. ACI Structural Journal. V. 118. No. 2. March 2021. doi: 10.14359/51729344.

[4] Guo H. Evaluation of column load for generally uniform grid-reinforced pile cap failing in punching. ACI Struct J 2015;112. https://doi.org/10.14359/51687420.

[5] Blévot J, Frémy R. Semelles sur pieux. Ann l'Institut Tech Du Bâtiment Des Trav Publics, 20(230), p. 223-295, Fev. 1967.

[6] Clarke JL. Behaviour and design of pile caps with four pile caps. Cem Concr Assoc 1973.

[7] Adebar P, Kuchma D, Collins MP. Strut-and-tie models for the design of pile caps: an experimental study. ACI Struct J, v.87, n. 01, p. 81-92, Jan-Feb. 1990.

[8] Suzuki K, Otsuki K, Tsubata T. Influence of bar arrangement on ultimate strength of four-pile caps. Trans Japan Concr Inst 1998;20:195–202.

[9] Suzuki K, Otsuki K, Tsubata T. Experimental study on four pile caps with taper. Trans Japan Concr Inst 1999;21:327–34.

[10] Suzuki K, Otsuki K, Tsuchiya T. Influence of edge distance on failure mechanisms of pile caps. Trans Japan Concr Inst 2000;22:361–8.

[11] Suzuki K, Otsuki K. Experimental study on corner shear failure of pile caps. Trans Japan Concr Inst 2002;23:303–10.

[12] Dey S, Karthik MM. Modeling four-pile cap behavior using three-dimensional compatibility strut-and-tie method. Eng Struct 2019;198:109499. https://doi.org/10.1016/j.engstruct.2019.109499.

[13] Miguel-Tortola L, Pallarés L, Miguel PF. Punching shear failure in three-pile caps: influence of the shear span-depth ratio and secondary reinforcement. Eng Struct 2018;155:127–43. https://doi.org/10.1016/j.engstruct.2017.10.077.

[14] Park J, Kuchma DA, Souza RA. Strength Predictions of Pile Caps by a Strut-and-Tie Model Approach. Canadian Journal of Civil Eng 2008;35(12):1399–413. https://doi.org/10.1139/L08-062.

[15] Souza R, Kuchma D, Park J, Bittencourt T. Adaptable strut-and-tie model for design and verification of four-pile caps. ACI Struct J 2009;106(2):142–50. https://doi.org/10.14359/56352.

[16] Chetchotisak P, Yindeesuk S, Teerawong J. Interactive strut-and-tie model for shear strength prediction of RC pile caps. Comput Concr 2017;Vol. 20. No. 3. https://doi.org/10.12989/cac.2017.20.3.329.

[17] AFNOR. DTU P18-702 BAEL 91 (revises 99). Règles techniques de conception et de calcul des ouvrages et constructions en béton armé suivant la méthode des états limites. Fascicule 62. titre 1er du CCTG – Travaux section 1 : béton armé ; February 2000.

[18] Adebar P, Zhou Z. Design of deep pile caps by strut-and-tie models. ACI Struct J 1996;93:437–48. https://doi.org/10.14359/9703.

[19] Cavers W, Fenton GA. An Evaluation of Pile Cap Design Methods in accordance with the Canadian Design Standard. Can J Civ Eng 2004;31(1):109–19. https://doi.org/10.1139/l03-075.

[20] ACI committee 318. Building code requirements for structural concrete and commentary (ACI 318-14). American Concrete Institute. Detroit. USA; 2014.

[21] Institute CRS. CRSI Handbook. IL: Schaumburg; 2008.

[22] Abaqus version 2012. theory manual. (2012). section 4.5.2. Damaged plasticity model for concrete and other quasi-brittle materials.

[23] Fédération Internationale du Béton. "Model Code 2010." Laussanne. Switzerland. 2013. doi:10.1002/9783433604090.